Chemical Geology xxx (2011) xxx–xxx

Contents lists available at ScienceDirect

Chemical Geology

journal homepage: www.elsevier.com/locate/chemgeo

Research paper

Monitoring the fate of copper nanoparticles in river biofilms using scanning transmission X-ray microscopy (STXM)

John R. Lawrence [a,*], James J. Dynes [b], Darren R. Korber [c], George D.W. Swerhone [a], Gary G. Leppard [d], Adam P. Hitchcock [e]

[a] Environment Canada, 11 Innovation Blvd., Saskatoon, SK, Canada, S7N 3H5
[b] Canadian Light Source Inc., 101 Perimeter Road, Saskatoon, SK. Canada, S7N 0X4
[c] Food and Bioproducts Sciences, University of Saskatchewan, Saskatoon, SK, Canada, S7N 5A8
[d] Environment Canada, PO Box 5050, Burlington, ON, Canada, L7R 4A6
[e] Brockhouse Institute for Materials Research, McMaster University, Hamilton, ON, Canada, L8S 4M1

ARTICLE INFO

Article history:
Received 7 October 2010
Received in revised form 18 July 2011
Accepted 19 July 2011
Available online xxxx

Keywords:
Scanning transmission X-ray microscopy
STXM
Bacteria
Biofilms
Copper
Nanomaterials/nanoparticles

ABSTRACT

Scanning transmission X-ray microscopy (STXM) at the C 1s and Cu 2p edges was used to study the fate of Cu nanoparticles, including their sorption–dissolution, speciation and distribution in a complex natural river biofilm exposed to 1 mg L^{-1} Cu nanoparticles for 5 min, 3 days or 7 days. The original Cu nanoparticles, ~30 nm in diameter, were composed of Cu(I) and Cu(II) species, presumably a Cu(I) core surrounded by oxidized Cu(II). When the Cu nanoparticles were initially added to the biofilm, Cu nanoparticles were occasionally found as individual particles but most frequently were observed as aggregates. The aggregates were in association with diatoms and the extracellular polymeric substances (EPS) of the biofilm. In addition, a new Cu(II) species, as evident from a shift in its peak position (−0.4 eV) relative to the Cu nanoparticles, was found to be sorbed by the diatoms after 5 min and was still detected after 7 days. Evidently, the Cu nanoparticles had undergone dissolution, followed by sorption of ionic Cu(II) by the diatoms. The bacteria and cyanobacteria in the biofilm did not apparently sorb detectable amounts of Cu at any time. C 1s measurements indicated that the Cu(II) from solution was sorbed by the lipid-rich extracellular polymeric substances associated with the diatoms. These observations demonstrated that both the Cu nanoparticles and dissolution products remained associated with the river biofilm through interactions with specific biopolymers up to 7 days following exposure. Therefore, for some metal nanomaterials, sorption of the solid phase with subsequent dissolution and re-sorption are significant with respect to their chemodynamics and effects on the biofilm, especially when trophic transfer events are considered. Importantly, these interactions provide an entry point for copper into the aquatic food web.

1. Introduction

The large-scale commercial production of nanoparticles (NP, defined for this work as those with at least one dimension <100 nm) that is occurring or is planned could result in releases of nano- to microgram levels in receiving environments based on estimates of 620 kg/y for nanosilver and 47,300 kg/y for TiO_2 entering the surface waters of Switzerland (Mueller and Nowack, 2008). In particular, copper-containing nanoparticles are among those with a wide range of actual and intended applications. These include catalytic uses of CuO (Zhou et al., 2006), heat transfer fluids (Chang et al., 2005), wood preservation (Cox, 1991), and as antimicrobials (Gabbay et al., 2006; Ren et al., 2009). Indeed, an entire range of copper-impregnated textiles is available for use in garments, bedding, and sportswear. Such applications imply that metal nanoparticles could enter aquatic systems through direct discharges, and from industrial, as well as domestic, wastewater effluents (Christen, 2007; Lovern et al., 2007). Thus, the environmental fate and potential toxicity of nanoparticles is of concern.

As has been noted in a wide variety of studies (Haak and McFeters, 1982; Lawrence et al., 2004; Battin et al., 2008), microorganisms are positioned at the base of the food web, where they drive most biogeochemical cycles and so-called ecosystem services. Microbial biofilms and flocs are also among the most reactive materials in aquatic systems, serving as extensive natural sinks for metals (Dynes et al., 2006b), pesticides (Wolfaardt et al., 1994), antimicrobial agents (Dynes et al., 2006a), and a variety of other environmental contaminants. Based on this and the observations of Liu et al. (2007) regarding apparent scavenging of nanoparticles by bacterial extracellular polymeric substances (EPS), Battin et al. (2009) suggested that biofilms may be exposed to higher levels of nanoparticles than

* Corresponding author at: Environment Canada, 11 Innovation Blvd., Saskatoon, Saskatchewan, Canada, S7N 3H5. Tel.: +1 306 975 5789; fax: +1 306 975 5143.
E-mail address: John.Lawrence@ec.gc.ca (J.R. Lawrence).

0009-2541/$ – see front matter.
doi:10.1016/j.chemgeo.2011.07.013

planktonic communities. Thus, there is the concern that the direct uptake of metal or metal oxide nanoparticles by microorganisms may occur, and relative to the dissolved ionic forms, their ecotoxicological effects may be enhanced. Also, because of the nanoparticles morphology, surface area, surface charge and coatings they may be more readily retained by microbial biofilms compared to the ionic forms of the metals, providing direct interactions with microbial cells. Furthermore, the dissolution of metal or metal oxide nanoparticles, and the subsequent uptake of metallic ions may account, at least in part, for the toxicity of nanoparticles. Hence, microbial exposure may continue for long periods of time as the nanoparticles serve as a point source for the ionic forms (Franklin et al., 2007; Heinlaan et al., 2008; Aruoja et al., 2009). Thus, there is the need to understand the interactions and biological impacts of nanoparticles dispersed in the environment, including their environmental exposure and bioaccumulation in microbial biofilms.

Tiede et al. (2008, 2009) pointed out that it would be valuable to focus research efforts on the release of nanomaterials, their behavior under a range of environmental conditions including pH, oxygen, nutrients etc., and their mobility, aggregation, complexation, adsorption behaviors to provide a basis for ecotoxicological studies. As such, methods are required to evaluate these behaviors. A number of methods have been reviewed recently (Domingos et al., 2009; Tiede et al., 2008) citing their advantages and disadvantages in various applications. Although widely recognized (Thieme et al., 2007), to date STXM has been largely overlooked as a tool in environmental and toxicological studies of nanomaterials. STXM offers many advantages, including: i) spatial resolution of <25 nm, ii) no requirement for sectioning or staining, iii) the optimal sample thickness may be as much as 10 μm in a hydrated state, iv) image contrast is based on the X-ray absorption properties of the sample itself, and v) it is capable of determining and quantitatively mapping metal species and the organochemical composition of biofilms (Lawrence et al., 2003; Benzerara et al., 2004; Bluhm et al., 2006; Dynes et al., 2006a,b; Hitchcock et al., 2009; Obst et al., 2009). The method also has the advantage of reduced radiation damage relative to transmission electron microscopy-based electron energy loss spectromicroscopy (Hitchcock et al., 2008). It is essential to study the behavior of nanoparticles in the context of complex microbial communities over extended periods of time and at the appropriate scale. STXM has been used recently to investigate the fate of nanoparticles in human skin (Graf et al., 2009). Here we report the use of STXM at the C 1s and Cu 2p edges to examine Cu nanoparticle sorption, speciation and distribution in a complex natural river biofilm under a variety of timed exposure regimes.

2. Materials and methods

2.1. Microcosm operation

The experimental set-up and reactor design for biofilm development has been described in detail previously (Lawrence et al., 2000, 2004). Natural river water (South Saskatchewan River, Saskatoon, SK, Canada) was used as inoculum and as a source of carbon and nutrients. The reactors were maintained at 21 ± 2 °C. The water was pumped through the reactors at a rate of 500 mL per day (one reactor volume) by using a multichannel peristaltic pump (Watson Marlow, Wilmington, MA.). At the end of 60 days, the polycarbonate slides, with attached biofilms, were removed from the reactor, at which time the slides covered in river water were exposed to 1 mg L^{-1} Cu nanoparticles for 5 min, 3 days or 7 days, before removal and rinsing (3× with sterile tap water) to remove all but sorbed Cu nanoparticles. After the incubation, all of the biofilm material (~40 μm thick) was aseptically scraped from the entire slide (11 cm^2) with a sterile silicone spatula and placed in a sterile 1-mL centrifuge tube. No homogenization of the sample was undertaken as the goal was to look at biofilms in as intact a condition as possible.

2.2. Scanning transmission X-ray microscopy and data analysis

All STXM samples were prepared by deposition of 1–5 μL of the biofilm material onto Si_3N_4 windows (1 × 1 mm, thickness 100 nm on a 200 μm thick chip, 5 × 5 mm, Norcada Inc., Edmonton, Canada). After the droplet was placed, the sample was air-dried within a few minutes on the stage of a stereo microscope (Dynes et al., 2006a,b). All samples were analyzed by confocal laser microscopy which allowed for the selection of representative biofilm areas which could be then systematically analysed using STXM. At least 3 representative areas from each of the 5 min, and 3 and 7 days systems were examined using STXM.

STXM at the Cu 2p and C 1s edges was performed on the spectromicroscopy beamline 10ID-1 at the Canadian Light Source (CLS), Saskatoon, SK, Canada (Kaznatcheev et al., 2007). The beamline was operated at an energy resolving power $E/\Delta E \geq 3000$. All samples were analyzed in 1/6 atmosphere of He. The as-measured transmitted signals were converted to optical densities (OD, absorbance) using incident flux measured through regions of the window devoid of biofilm, to correct for the absorbance by the silicon nitride window. After each analytical measurement, an image was recorded at 289 eV, an energy which readily visualizes radiation damage to polysaccharides, the most easily-affected chemical component. The extracellular matrix polysaccharide signal was reduced by less than 20% in the worst case of the measurements reported. The C 1s energy scale was calibrated to an accuracy of ± 0.05 eV using the Rydberg peaks of CO_2. The absolute energy scale of the Cu L-edge region was set by assigning the energy of the primary peak of the L_3-edge of CuO to 931.3 eV (Grioni et al., 1989b). STXM was used analytically by measuring image sequences at specific energies (Jacobsen et al., 2000) and fitting these image sequences to linear combinations of reference spectra of components suspected to be present in the biofilm using singular value decomposition (SVD) or from image difference maps which are the difference of on- and off-resonance images (Dynes et al., 2006a). Data analysis was performed using aXis2000 (Hitchcock, 2011). The colocalization analysis was conducted using ImageJ (WCIF, 2011).

2.3. Reference spectra

The spectra of CuO, Cu_2O and Cu metal were used to identify the oxidation state of the Cu nanoparticles. CuO and Cu acetate were obtained from Sigma-Aldrich, while the Cu_2O was obtained from Alfa Aesar, and all were >99% pure. The CuO, Cu acetate and Cu_2O powders were slurried in water and deposited onto silicon nitride windows and air-dried before STXM analysis. The fluorescence yield spectrum of Cu metal was determined from the Cu holder on the CLS spherical grating monochromator beamline 11ID-1. The spectra of the major biomacromolecules (protein, lipids, polysaccharides) used to fit the C 1s image sequences are shown in Fig. S1 and were discussed previously (Dynes et al., 2006a). The Cu acetate reference spectrum was placed on an absolute linear absorbance scale by matching it to the predicted response for the compound based on its elemental composition and density (1.88 g cm^{-3}) using tabulated continuum absorption coefficients (Henke et al., 1993).

2.4. Confocal laser scanning microscopy (CLSM)

CLSM images were collected using an MRC 1024 confocal laser scanning microscope (Bio-Rad, Hemel Hempstead, United Kingdom) attached to a Microphot SA microscope (Nikon, Tokyo, Japan) equipped with a 40×, 0.55 numerical aperture (NA) (Nikon), 10×, 0.3 NA (Nikon) and 63×, 0.9 NA lens (Zeiss, Jena, Germany) as described previously (Lawrence et al., 2003; Dynes et al., 2006a). All samples were analyzed

Please cite this article as: Lawrence, J.R., et al., Monitoring the fate of copper nanoparticles in river biofilms using scanning transmission X-ray microscopy (STXM), Chem. Geol. (2011), doi:10.1016/j.chemgeo.2011.07.013

by confocal laser microscopy (Bio-Rad MRC 1024, Zeiss, Jena, Germany) using the fluorescent stains Syto9 (Molecular Probes, Eugene, OR) and *Triticum vulgaris* lectin-TRITC (Sigma, St. Louis, MI). SYTO 9 (excitation/emission 488/522 nm) targets the nucleic acids of bacteria and is recorded in the green channel. *T. vulgaris* (excitation/emission 568, 605/32 nm) targets the EPS of the biofilm and is recorded in the red channel. The photosynthetic organisms (i.e., algae, cyanobacteria) autofluoresce (excitation/emission 647/680 nm) and are recorded as the blue channel (Neu et al., 2004). Cyanobacteria also autofluoresce (excitation/emission 568, 605/32 nm) and are also recorded in the red channel.

3. Results

3.1. Characterization of Cu nanoparticles

The Cu L_3-edge spectra of the Cu nanoparticles, as well as that of CuO (formally Cu(II)), Cu_2O (formally Cu(I)) and Cu metal (formally Cu(0)) measured in STXM are shown in Fig. 1. The CuO, Cu_2O and Cu metal Cu L_3-edge spectra are similar to that reported previously (Grioni et al., 1989a,b; Todd and Sherman, 2003). Note that the peak at about 931 eV in the Cu_2O spectra is due to Cu(II) contamination. Comparison of the Cu L_3-edge spectra of the Cu nanoparticles to that of the Cu(II), Cu(I) and Cu(0) reference spectra showed that, prior to incorporation into the biofilm, the Cu nanoparticles were a composite of Cu(II) and Cu(I) oxidation states. Pattrick et al. (1993) showed that the intensity of the Cu(II) edge in minerals is approximately 25 times that of the Cu(I) edge; therefore, compounds containing both Cu(I) and Cu(II) will be dominated by contributions from the Cu(II). Hence, it is likely that the Cu nanoparticles were predominantly Cu(I) with some Cu(II) on the surface. The Cu nanoparticles were found to be non-crystalline by powder X-ray diffraction analysis.

3.2. Interaction of Cu nanoparticles with the river biofilm

A CLSM image of a typical river biofilm from this study is shown in Fig. 2. River biofilms in this study are a complex community of microorganisms, composed of bacteria, cyanobacteria, diatoms and EPS. The natural Cu concentration in South Saskatchewan River water is 0.003 mg L^{-1} (City of Saskatoon website). In a control biofilm which was not exposed to Cu nanoparticles, a Cu NEXAFS signal could not be detected in the EPS, diatoms, cyanobacteria or bacteria; thus, any Cu detected in the biofilm, in addition to the Cu nanoparticles is assumed to have originated from the Cu nanoparticles.

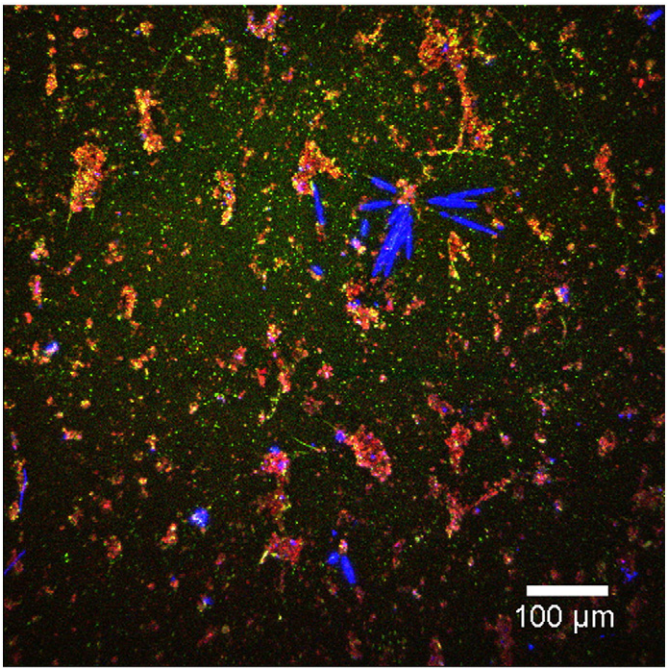

Fig. 2. Confocal laser scanning microscopy (CLSM) micrograph of a river biofilm grown in the presence of Cu nanoparticles showing the typical appearance and distributions of algae (e.g., diatoms, blue), cyanobacteria (magenta), bacteria (green, yellow) and EPS (red). The biofilm was stained with *T. vulgaris* (red) and SYTO 9 (green). Autofluorescence of algae is recorded as blue; cyanobacteria are recorded as blue and red.

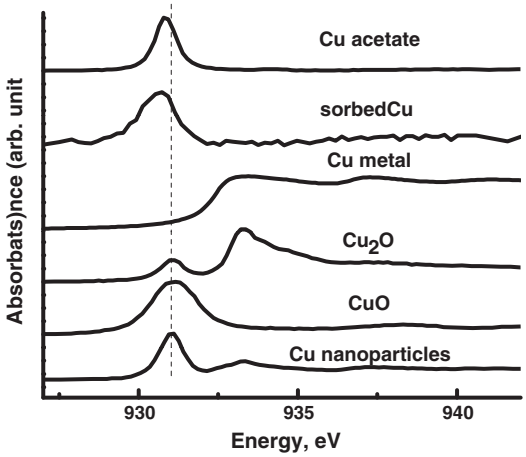

Fig. 1. Cu $2p_{3/2}$-edge spectra of Cu nanoparticles, CuO, Cu_2O, Cu metal, Cu acetate and Cu sorbed by the biofilm. All of the spectra were collected as transmission, except the Cu metal which was collected as fluorescence yield. The sorbed Cu spectrum was obtained by masking of the pixels with high intensity from the sorbed Cu component map (Fig. S2e) from the diatom in Fig. 5.

The biofilm was exposed to 1 mg L^{-1} of Cu nanoparticles (Cu concentration about 0.85 mg L^{-1}) for 5 min, 3 days and 7 days. To determine the fate of Cu nanoparticles in the biofilm, detailed analyses were undertaken of selected microorganisms with distinct morphologies. For biofilms exposed to Cu nanoparticles for 5 min, Figs. 3a and 4a present a Cu map ($I_{931.3eV}$–I_{925eV}) (red) superimposed on a biology map ($I_{288.2eV}$–I_{280eV}) (gray scale). In each case aggregates of Cu nanoparticles are visible. Detailed analysis was conducted on a region of a pennate diatom (location indicated in Fig. 3a) and a cyanobacteria (location indicated in Fig. 4a) at the Cu 2p and C 1s edges to map the Cu NP in the context of the major biomacromolecules. The Cu NP used in this study released 0.06 mg L^{-1} from 1 mg L^{-1} Cu NP in river water. Hence, the Cu 2p edge was also used to look for sorbed Cu species. A Cu 2p image sequence was collected on a region of the pennate diatom in Fig. 3a. It was possible to manually extract a Cu spectrum similar to that of the reference Cu NP from obvious aggregates of Cu NP. In addition, another Cu spectrum from the diatom, consisting of a single peak shifted nearly 0.4 eV lower than the Cu(II) peak in the spectrum of the original Cu nanoparticles was obtained. The energy peak position has been shown to shift to lower energy for Cu compounds containing different ligands (e.g., CO_3^{2-}, SO_4^{2-}, SiO_3) compared to CuO (van der Laan et al., 1992), as was the case for Cu acetate (−0.4 eV) (Fig. 1). This new Cu species consisted only of Cu(II), lacking the peak around 933 eV which is characteristic of Cu(I) species (Grioni et al., 1989a,b). This new Cu(II) species was considered to be a sorbed form of Cu(II), presumably Cu from the dissolution of the Cu NP, and is hereafter referred to as "sorbed Cu" and its spectrum is shown in Fig. 1. The fact that the sorbed Cu species did not contain any Cu(I) supports the contention that Cu(II) ions from solution were sorbed by the diatom. Given the pH and oxidation state of the river water, Cu(I) ions would not be expected to persist. Spectral fitting using the Cu NP reference and Cu acetate spectra (Fig. 1) was conducted on the Cu 2p image sequence of a region of the diatom in Fig. 3a using SVD analysis. The Cu acetate

Please cite this article as: Lawrence, J.R., et al., Monitoring the fate of copper nanoparticles in river biofilms using scanning transmission X-ray microscopy (STXM), Chem. Geol. (2011), doi:10.1016/j.chemgeo.2011.07.013

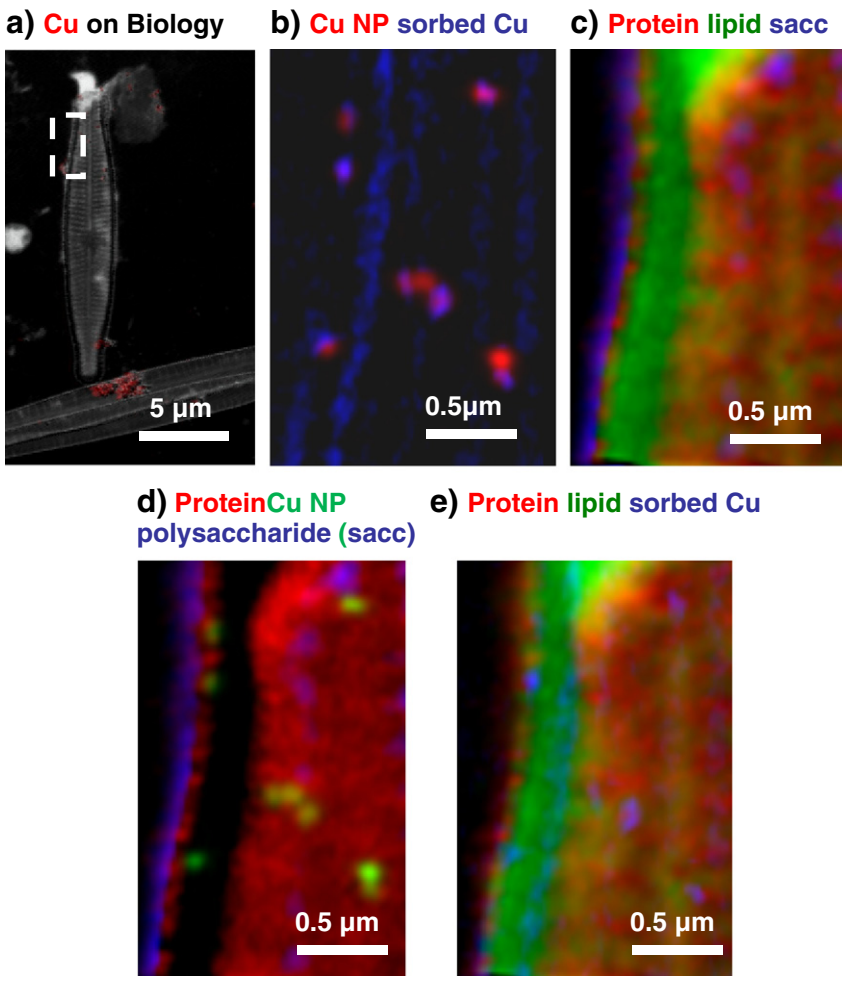

Fig. 3. Detailed study of a diatom (area in white box) from the river biofilm exposed to 1 mg L^{-1} Cu nanoparticles (NP) for 5 min. (a) Cu image difference map ($I_{931.3eV}$–I_{925eV}) (red) overlayed on the gray scale of the biology image difference map ($I_{288.2eV}$–I_{280eV}). (b) Color-coded composite map of Cu nanoparticles (red) and sorbed Cu (blue). (c) Color-coded composite map of protein (red), lipid (green) and polysaccharides (blue). (d) Color-coded composite map of protein (red), Cu NP (green) and polysaccharides (blue). (e) Color-coded composite map of protein (red), lipid (green) and sorbed Cu (blue).

spectrum was similar to the sorbed Cu in that it contained a L_3-edge single peak, thus it was used in place of the sorbed Cu spectrum to estimate the amount of sorbed Cu in the biofilms. Since the exact formula of the sorbed Cu was unknown, using the Cu acetate spectrum may result in a systematic quantitation error, by as much as 50% (Dynes et al., 2006b). The overlay of the Cu NP and sorbed Cu component maps (Fig. S2) is shown in Fig. 3b. Cu nanoparticles were apparently in association with the diatom in no set pattern, while sorbed Cu was distributed over the entire diatom, particularly as a strip parallel to the edge of the diatom frustules. The average effective thickness of sorbed Cu by the diatom was 1.1 ± 1.4 nm. The C 1s edge provides information on the composition of the matrix with which the nanomaterials are associated, allowing the metal or other nanomaterials to be placed in a biological context (Dynes et al., 2006b). Spectral fitting of the C 1s image sequence with spectra of the major biomacromolecules (protein, lipid, polysaccharides, CO_3^{2-}, K^+) (Fig. S1) was performed to map their distribution in the biofilm. Fig. 3c shows the distribution of protein, lipids and polysaccharides in this region of the diatom, derived from their individual component maps (Fig. S2). The polysaccharides were mainly concentrated on the edge of the diatom, with some localized regions on the diatom. The protein was distributed over much of the diatom, except in a region where lipids were highly localized (Fig. 3), although lipids were also distributed over the entire diatom. Other researchers (Kröger et al., 1999; Kainz et al., 2009) have similarly shown that proteins and lipids are major biomolecules in diatoms. Fig. 3d shows the overlap of the sorbed Cu component map (Fig. 3b) with the protein and lipid component maps (Fig. S2). Mander's overlap coefficients for the sorbed Cu with protein, lipids and polysaccharides were 0.732, 0.965 and 0.163, respectively, indicating that the sorbed Cu was associated predominantly with the lipids.

A Cu 2p image sequence was collected from a region of the cyanobacteria exposed to Cu NP for 5 min (Fig. 4a). Spectral fitting with the Cu NP and Cu acetate spectra (Fig. 1) was conducted using SVD analysis. It was not possible to obtain a "sorbed Cu" spectrum by masking the pixels identified from the sorbed Cu component map (not shown); thus, it appears that only Cu NP were present in the vicinity of the cyanobacteria. The Cu NP component map (Fig. S3) was generated from spectral fitting using the Cu NP spectrum. Spectral fitting of a C 1s image sequence from the same area of the Cu 2p image sequence was performed using the same biomacromolecule spectra as that used for the pennate diatom (Fig. S1) and SVD analysis. The color-coded overlap of the selected component maps (Fig. S1) are shown in Fig. 4b. The cyanobacterial filament was composed of protein and polysaccharides, surrounded by lipids, protein and polysaccharides. The color-coded overlay of the Cu NP component map with the lipid and protein component maps (Fig. S3) is shown in Fig. 4c. The Mander's overlap coefficient for the Cu NP with protein, lipid and polysaccharides was 0.681, 0.827 and 0.661, respectively, indicating that the Cu NP were mainly associated with the lipids external to the cells (Fig. 4c), and not directly associated with the cyanobacteria.

Please cite this article as: Lawrence, J.R., et al., Monitoring the fate of copper nanoparticles in river biofilms using scanning transmission X-ray microscopy (STXM), Chem. Geol. (2011), doi:10.1016/j.chemgeo.2011.07.013

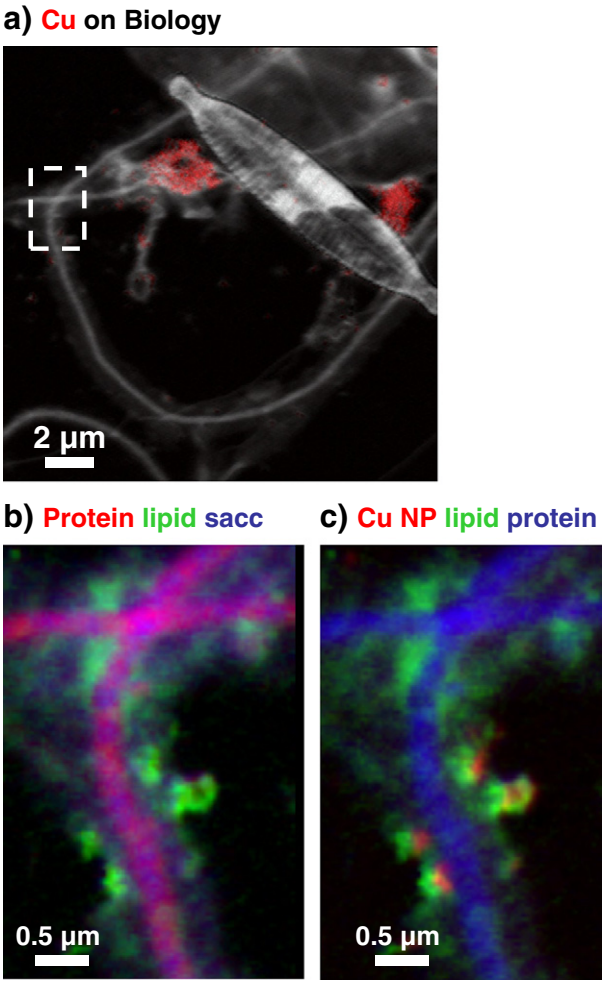

Fig. 4. River biofilm exposed to 1 mg L^{-1} Cu nanoparticles for 5 min. (a) Cu image difference map ($I_{931.3eV}$–I_{925eV}) (red) overlayed on the gray scale of the biology image difference map ($I_{288.2eV}$–I_{280eV}). The white box indicates the area of the detailed study. Detailed study of a cyanobacterial cell. (b) Color-coded composite map of protein (red), lipid (green) and polysaccharides (blue). (c) Overlay of the Cu image difference map from a on the lipid and protein component maps from b (red = Cu nanoparticles, green = lipid, blue = protein).

After 3 days of exposure to the Cu nanoparticles, aggregates of Cu nanoparticles were still evident in the biofilm (Fig. 5a). Collection of a Cu 2p image sequence of a region of a diatom, and subsequent spectral fitting with Cu NP and Cu acetate using SVD confirmed that Cu NP and sorbed Cu were associated with the diatom (Fig. 5b, Fig. S4). The Cu NP were sorbed in no set pattern. The sorbed Cu was distributed over most of the diatom, except in an area near the edge of the diatom frustule. The average effective thickness of sorbed Cu by the diatom was 1.0 ± 1.5 nm. A C 1s image sequence of the same region as the Cu 2p image sequence and SVD analysis using the biomacromolecule spectra (Dynes et al., 2006a) showed that protein, lipids and polysaccharides were present in the diatom (Fig. S4). Overlay of the protein, lipid and polysaccharide component maps (Fig. 5c, Fig. S4) showed that polysaccharides and proteins were on the edge of the diatom and in the center of the diatom frustules, while lipids were distributed over the entire diatom. The sorbed Cu component map was overlayed on the lipid and polysaccharide component maps (Fig. 5d, Fig. S4). Mander's overlay coefficients indicated that the sorbed Cu was chiefly associated with the lipids (0.851) but also with the protein (0.772) and polysaccharides (0.758). SVD analysis of image sequences at the Cu 2p edge using the Cu NP and sorbed Cu spectra (Fig. 1) of bacteria exposed to the Cu nanoparticles for 3 days indicated that bacteria did not sorb detectable amounts of Cu.

After 7 days, Cu nanoparticles were no longer visible in the biofilm (Fig. 6a). A Cu 2p stack on a region of a diatom and adjacent bacteria was collected and analyzed using the Cu NP and Cu acetate spectra by SVD analysis. Only a sorbed Cu spectrum could be extracted using the component maps to guide the selection of pixels, indicating that Cu NP were no longer associated with the diatom, presumably the Cu NP completely dissolved as supported by the disappearance of the Cu(I) peak at 933 eV. The sorbed Cu was mainly concentrated on the edges of the diatom. The average effective thickness of sorbed Cu by the diatom was 1.5 ± 1.5 nm. Fig. 6c shows the distribution of the major biomacromolecules in the diatom from overlay of the protein, lipid and polysaccharide component maps (Fig. S5). Also, a spectrum was extracted from regions of the protein, lipid and polysaccharide component maps with high intensity pixels to confirm that these biomacromolecules were present in the biofilm (Fig. S1) (Dynes et al., 2006a,b). Overlap of the sorbed Cu component map (Fig. 6b) with the lipid and protein component maps (Fig. S5) was shown in Fig. 6d. Mander's overlap coefficients for the sorbed Cu with protein, lipids and polysaccharides were 0.577, 0.865 and 0.662, respectively, thus the sorbed Cu continued to be mainly associated with the lipids but also with the proteins and polysaccharides. The bacteria next to the diatom did not sorb detectable amounts of Cu. Examination of other bacteria and cyanobacteria in the biofilm exposed to Cu NP for 7 days did not show any sorbed Cu associated with these morphological types.

4. Discussion

A key aspect of understanding the impact of nanoparticles released into the environment is to examine the interaction between nanoparticles and microorganisms, which are not only highly abundant in nature but critical for global environmental processes (Aruguete and Hochella, 2010). It has been suggested that nanoparticles would aggregate and sorb onto the surfaces of aquatic sediments, algal mats, biofilms and soils (Handy et al., 2008a,b; Battin et al., 2009). Our observations suggest that Cu nanoparticles entering the aquatic environment will either be aggregates or undergo aggregation; biological structures such as biofilms may serve as a sorbent for nanoparticles and aggregates. Gao et al. (2009) examined the aggregation of Cu nanoparticles in natural river water and observed that enhanced aggregation of Cu nanoparticles could be attributed to the effect of high electrolyte and low dissolved organic carbon concentrations, conditions similar to those found in Saskatchewan River water. Most frequently, the Cu nanoparticle aggregates in this study were found in association with specific biomaterials such as lipids in the vicinity of cyanobacteria and on diatoms. Biofilm and cell surfaces are dominated by polyanionic EPS and ligands (Neu and Lawrence, 2009) which could sorb nanoparticle aggregates, creating higher concentrations of nanomaterials on the surface of the organism relative to that in the bulk water.

Research has shown that microorganisms sorb Cu ions from solution and that Cu NP can be sources of Cu ions (Aruoja et al., 2009; Blinova et al., 2010). The Cu nanoparticles used in this study were initially suspended in river water before being added to the biofilms, which resulted in their partial dissolution (0.06 mg Cu L^{-1}). After 5 min exposure to the Cu nanoparticles, a new Cu(II) species was found to be sorbed by the diatoms in the biofilm. The cell walls of diatoms are semi-permeable allowing for the passage of small molecules, while limiting the passage of larger molecules. It has been suggested that small nanoparticles or nanoparticle aggregates may pass through the cell wall and reach the plasma membrane (Navarro et al., 2008). Further, the diatom frustule is about 97% hydrated silica (SiO_2) (Noll et al., 2002), thus, it is possible that some sorbed Cu is directly bound on the silica. The 3D spatial distribution of Cu in a diatom (*Cyclotella meneghiniana*) grown in growth media containing $CuSO_4$ was examined using X-ray fluorescence 3D

Please cite this article as: Lawrence, J.R., et al., Monitoring the fate of copper nanoparticles in river biofilms using scanning transmission X-ray microscopy (STXM), Chem. Geol. (2011), doi:10.1016/j.chemgeo.2011.07.013

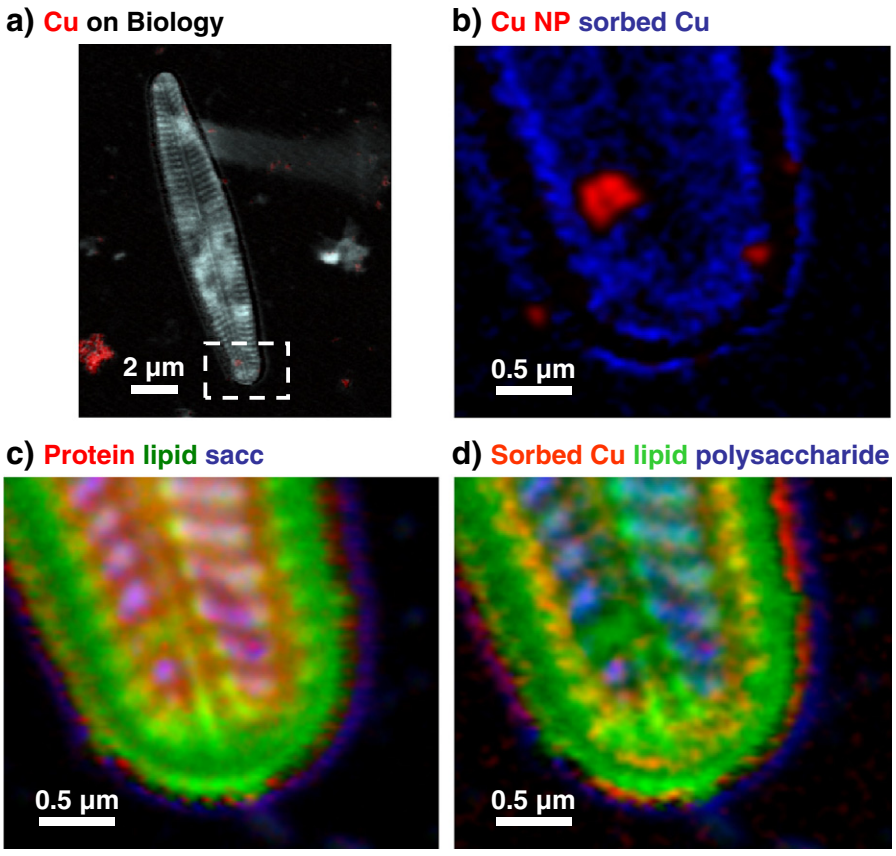

Fig. 5. Detailed study of a diatom (area in white box) from the river biofilm exposed to 1 mg L^{-1} Cu nanoparticles for 3 days. (a) Cu image difference map ($I_{931.3eV}$–I_{925eV}) (red) overlayed on the gray scale of the biology image difference map ($I_{288.2eV}$–I_{280eV}). (b) Color-coded composite map of Cu nanoparticles (red) and sorbed Cu (blue). (c) Color-coded composite map of protein (red), lipid (green) and polysaccharides (blue). (d) Overlay of the sorbed Cu (red) and lipid (green) and protein (blue) component maps.

microtomography (de Jonge et al., 2010). The Cu was found to be mainly in a thin layer of cytoplasm along the inside of the diatom frustules and in a cytoplasmic pillar running along the axis of the diatom. It is likely that the new Cu(II) species sorbed by the diatoms in this study also resided in the thin layer of cytoplasm on the inside of the diatom frustules and not on the silica of the frustules. Also, it was likely that the nanoparticles did not pass through the cell walls and dissolve inside the cell but that dissolution occurred external to the cell. This is because the solubility of the Cu nanoparticles used in this study in river water was low (0.06 mg Cu L^{-1}). Hence, it is unlikely that within a 5 min period the Cu nanoparticles passed through the cell wall, dissolved completely such that all the Cu(I) was converted to Cu(II) and that the ionic Cu(II) species were sorbed by the diatom. It is more probable that the partial dissolution of the Cu nanoparticles occurred when they were initially suspended in the river water, and it was the ionic Cu(II) species that were sorbed by the diatom cytoplasm. Other researchers (Heinlaan et al., 2008; Aruoja et al., 2009; Blinova et al., 2010; Ganesh et al., 2010) have attributed the toxicity of Cu nanoparticles to microorganisms to the solubilised Cu ions. The apparent lack of transfer of Cu nanoparticles into the cell implies a potential reduction in effect at the cellular level, although surface-acting toxicity may be a factor (Neal, 2008). Indeed, we have observed significant reductions in cellular biomass and algal abundance in parallel studies on the river biofilm community structure and function (Lawrence et al. unpublished data).

Cu nanoparticles were no longer observed to be present in the biofilm after 7 days, presumably because they had completely dissolved, and all the Cu(I) was oxidized to Cu(II). This suggests that Cu nanoparticles released into aquatic systems may not persist in the environment. In this study, the diatoms served as a sink for the ionic Cu species. The average effective thickness of Cu sorbed by the diatoms was relatively constant at about 1 .3 ± 1.5 nm in the 5 min and 3 and 7 days Cu exposed biofilms.

The bacteria and cyanobacteria were not observed to sorb Cu in this study. Pokrovsky et al. (2008) observed that within 1 min both pure cultures of bacteria and cyanobacteria sorbed Cu; the Cu concentration range was 0.1 to 10–100 µM versus about 1 µM Cu (in solution) in this study. One possible reason that Cu was not observed to be sorbed by the bacteria and cyanobacteria may be that the amount sorbed was below the detection limit of STXM. Another possibility was that the diatoms served as a "natural sink", removing the Cu from solution before significant amounts could be sorbed by the bacteria and cyanobacteria. In any case, in a mixed river biofilm, diatoms appear to be the most significant Cu sorbent.

These results demonstrate that STXM can be used to acquire information on nanomaterials and their interactions with natural microbial biofilm communities. We have been able to show localization and speciation of copper nanoparticles in the biofilm, confirming sorption, dissolution and sorption as Cu(II) forms in and on diatoms. Our soft X-ray spectromicroscopy analyses of river biofilm communities indicated that when copper nanoparticles, and likely other metal nanomaterials, enter an aquatic environment they may follow several pathways, including: i) aggregation, ii) sorption to the biota as single nanoparticles or as aggregates, iii) transformation to copper oxides, iv) sorption and/or resorption to the biota, v) dissolution with the formation of ionic copper species, vi) subsequent sorption or uptake by selected microbial species in biofilms, and vii) trophic transfer to organisms grazing on the biofilms or community members.

Please cite this article as: Lawrence, J.R., et al., Monitoring the fate of copper nanoparticles in river biofilms using scanning transmission X-ray microscopy (STXM), Chem. Geol. (2011), doi:10.1016/j.chemgeo.2011.07.013

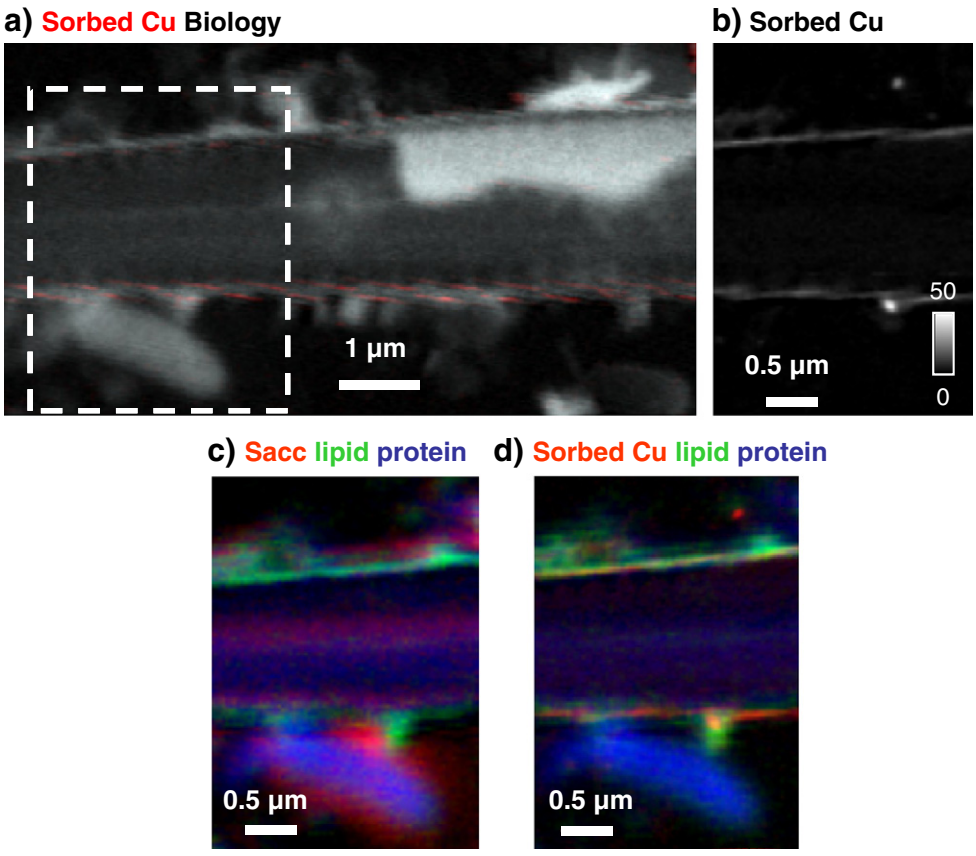

Fig. 6. Detailed study of a diatom (area in white box) from the river biofilm exposed to 1 mg L^{-1} Cu nanoparticles for 7 days. (a) Cu image difference map ($I_{931.3eV}$–I_{925eV}) (red) overlayed on the gray scale of the biology image difference map ($I_{288.2eV}$–I_{280eV}). (b) Gray scale composite map of sorbed Cu. The gray scale is the effective thickness in nm. (c) Color-coded composite map of protein (blue), lipid (green) and polysaccharides (red). (d) Overlay of sorbed Cu (red), lipid (green) and protein (blue) component maps.

Acknowledgments

This study was supported by Environment Canada, NSERC and the Canada Research Chair program (APH). Research described in this paper was performed at the Canadian Light Source, which is supported by the Natural Sciences and Engineering Research Council of Canada, the National Research Council Canada, the Canadian Institutes of Health Research, the Province of Saskatchewan, Western Economic Diversification Canada, and the University of Saskatchewan. We thank Chithra Karunakaran, Jian Wang and Yingshen Lu for their expert support of the spectromicroscopy facility at the CLS.

Appendix A. Supplementary data

Supplementary data to this article can be found online at doi:10.1016/j.chemgeo.2011.07.013.

References

Aruguete, D.M., Hochella Jr., M.F., 2010. Bacteria–nanoparticle interactions and their environmental implications. Environ. Chem. 7, 3–9.
Aruoja, V., Dubourguier, H.C., Kasemets, K., Kahru, A., 2009. Toxicity of nanoparticles of CuO, ZnO and TiO_2 to microalgae *Pseudokirchneriella subcapitata*. Sci. Tot. Environ. 407, 1461–1468.
Battin, T.J., Kaplan, L.A., Findlay, S., Hopkinson, C.S., Marti, E.M., Packman, A.I., Newbold, J.D., Sabater, F., 2008. Biophysical controls on organic carbon fluxes in fluvial networks. Nat. Geosci. 1 (2), 95–100.
Battin, T.J., Kammer, F.V.D., Weilhartner, A., Ottofuelling, S., Hofmann, T., 2009. Nanostructured TiO_2: transport behavior and effects on aquatic microbial communities under environmental conditions. Environ. Sci. Technol. 43, 8098–8104.
Benzerara, K., Yoon, T.H., Tyliszczak, T., Constantz, B., Spormann, A.M., Brown, G.E., 2004. Scanning transmission X-ray microscopy study of microbial calcification. Geobiology 2, 249–259.
Blinova, I., Ivask, A., Heinlaan, M., Mortimer, M., Kahru, A., 2010. Ecotoxicity of nanoparticles of CuO and ZnO in natural water. Environ. Pollut. 158, 41–47.
Bluhm, H., Andersson, K., Araki, T., Benzerara, K., Brown, G.E., Dynes, J.J., Ghosal, S., Gilles, M.K., Hansen, H.-C.h., Hemminger, J.C., Hitchcock, A.P., Ketteler, G., Kilcoyne, A.L.D., Kneedler, E., Lawrence, J.R., Leppard, G.G., Majzlam, J., Mun, B.S., Myneni, S.C.B., Nilsson, A., Ogasawara, H., Ogletree, D.F., Pecher, K., Salmeron, M., Shuh, D.K., Tonner, B., Tyliszczak, T., Warwick, T., Yoon, T.H., 2006. Soft X-ray microscopy and spectroscopy at the molecular environmental science beamline at the advanced light source. J. Electron. Spectrosc. Relat. Phenom. 150, 86–104.
Chang, H., Jwo, C.S., Lo, C.H., Tsung, T.T., Kao, M.J., Lin, H.M., 2005. Rheology of CuO nanoparticle suspension prepared by ASNSS. Rev. Adv. Mater. Sci. 10, 128–132.
Christen, K., 2007. Nanomaterials meet increased scrutiny. Environ. Sci. Technol. News 41 (3), 671–672.
City of Saskatoon, http://www.saskatoon.ca.
Cox, C., 1991. Chromated copper arsenate. J. Pestic. Reform. 11, 2–6.
de Jonge, M.D., Holzner, C., Baines, S.B., Twining, B.S., Ignatyev, K., Diaz, J., Howard, D.L., Legnini, D., Miceli, A., McNulty, I., Jacobsen, C., Vogt, S., 2010. Quantitative 3D elemental microtomography of *Cyclotella meneghiniana* at 400-nm resolution. Proc. Natl Acad. Sci. 107, 15,676–15,680.
Domingos, R.F., Baalousha, M.A., Ju-Nam, Y., Marcia Reid, M., Tufenkji, N., Lead, J.R., Leppard, G.G., Wilkinson, K.J., 2009. Characterizing manufactured nanoparticles in the environment: multimethod determination of particle sizes. Environ. Sci. Technol. 43, 7277–7284.
Dynes, J.J., Lawrence, J.R., Korber, D.R., Swerhone, G.D.W., Leppard, G.G., Hitchcock, A.P., 2006a. Quantitative mapping of chlorhexidine in natural river biofilms. Sci. Total Environ. 369, 369–383.
Dynes, J.J., Tyliszczak, T., Araki, T., Lawrence, J.R., Swerhone, G.D.W., Leppard, G.G., West, M.M., Hitchcock, A.P., 2006b. Quantitative mapping of metal species in bacterial biofilms using scanning transmission X-ray microscopy. Environ. Sci. Technol. 40, 1556–1565.
Franklin, N.M., Rogers, N.J., Apte, S.C., Gadd, G.E., Casey, P.S., 2007. Comparative toxicity of nanoparticulate ZnO, bulk ZnO, and $ZnCl_2$ to a freshwater microalga (*Pseudokirchneriella subcaptata*): the importance of particle solubility. Environ. Sci. Technol. 41, 8484–8490.
Gabbay, J., Borkow, G., Mishal, J., Magen, E., Zatcoff, R., Shemer-Avni, Y., 2006. Copper oxide impregnated textiles with potent biocidal activities. J. Ind. Text. 35, 323–335.
Ganesh, R., Smeraldi, J., Hosseini, T., Khatib, L., Olson, B.H., Rosso, D., 2010. Evaluation of nanocopper removal and toxicity in municipal wastewaters. Environ. Sci. Technol. 44, 7808–7813.
Gao, J., Youn, S., Hovsepyan, A., Llandeza, V.L., Wang, Y., Bitton, G., Bonzongo, J.-C.J., 2009. Dispersion and toxicity of selected manufactured nanomaterials in natural

river water samples: effects of water chemical composition. Environ. Sci. Technol. 43, 3322–3328.
Graf, C.M., Meinke, M.C., Gao, Q., Hadam, S., Raabe, J., Sterry, W., Blume-Peytavi, U., Lademann, J.M., Ruhl, E., Vogt, A., 2009. Qualitative detection of single submicron and nanoparticles in human skin by scanning transmission x-ray microscopy. J. Biomed. Opt. 14 (021015), 1–6.
Grioni, M., Goedkoop, J.B., Schoorl, R., deGroot, F.M.F., Fuggle, J.C., Schäfers, F., Koch, E.E., Rossi, G., Esteva, J.-M., Karnatak, R.C., 1989a. Studies of copper valence states with Cu L_3 x-ray absorption spectroscopy. Phys. Rev. B 39, 1541–1545.
Grioni, M., Czyzyk, M.T., de Groot, F.M.F., Fuggle, J.C., Watts, B.E., 1989b. Unoccupied electronic states of CuO: an oxygen 1s X-ray absorption spectroscopy investigation. Phys. Rev. B 38, 4886–4890.
Haak, S.K., McFeters, G.A., 1982. Microbial dynamics of an epilithic mat community in a high alpine stream. Appl. Environ. Microbiol. 43, 702–707.
Handy, R.D., Owen, R., Valsami-Jones, E., 2008a. The ecotoxicology of nanoparticles and nanomaterials: current status, knowledge gaps, challenges, and future needs. Ecotoxicology 17 (5), 315–325.
Handy, R.D., Kammer, F.V.D., Lead, J.R., Hassell, M., Owen, R., Crane, M., 2008b. The ecotoxicology and chemistry of manufactured nanoparticles. Ecotoxicology 17 (5), 287–314.
Heinlaan, M., Ivask, A., Blinova, I., Dubourguier, H.C., Kahru, A., 2008. Toxicity of nanosized and bulk ZnO, CuO and TiO_2 to bacteria *Vibrio fischeri* and crustaceans *Daphnia magna* and *Thamnocephalus platurus*. Chemosphere 71, 1308–1316.
Henke, B.L., Gullikson, E.M., Davis, J.C., 1993. X-ray interactions—photoabsorption, scattering, transmission and reflection at E = 50–30,000 eV, Z = 1–92. Atomic Data Nuclear Data Tables 54, 181–297.
Hitchcock, A.P., 2011. aXis2000 is written in Interactive Data Language (IDL)It is available free for non-commercial use from http://unicorn.mcmaster.ca/aXis2000.html.
Hitchcock, A.P., Dynes, J.J., Johansson, G., Wang, J., Botton, G., 2008. Comparison of NEXAFS microscopy and TEM-EELS for studies of soft matter. Micron 39, 311–319.
Hitchcock, A.P., Dynes, J.J., Lawrence, J.R., Obst, M., Swerhone, G.D.W., Korber, D.R., Leppard, G.G., 2009. Soft X-ray spectromicroscopy of nickel sorption in a natural river biofilm. Geobiology 7, 432–453.
Jacobsen, C., Wirick, S., Flynn, G., Zimba, C., 2000. Soft X-ray spectroscopy from image sequences with sub-100 nm spatial resolution. J. Microsc. 197, 173–184.
Kainz, M.J., Perga, M.E., Arts, M.T., Mazumder, A., 2009. Essential fatty acid concentrations of different seston sizes and zooplankton: a field study of monomictic coastal lakes. J. Plankton Res. 31, 635–645.
Kaznatcheev, K.V., Karunakaran, C., Lanke, U.D., Urquhart, S.G., Obst, M., Hitchcock, A.P., 2007. Soft X-ray spectromicroscopy beamline at the CLS: commissioning results. Nucl. Instrum. Methods Phys. Res. Sect. A-Accel. Spectrom. Dect. Assoc. Equip. 582, 96–99.
Kröger, N., Deutzmann, R., Sumper, M., 1999. Polycationic peptides from diatom biosilica that direct silica nanosphere formation. Science 286, 1129–1132.
Lawrence, J.R., Swerhone, G.D.W., Neu, T.R., 2000. Design and evaluation of a simple rotating annular reactor for replicated biofilm studies. J. Microbiol. Meth. 42, 215–224.
Lawrence, J.R., Swerhone, G.D.W., Leppard, G.G., Araki, T., Zhang, X., West, M.M., Hitchcock, A.P., 2003. Scanning transmission x-ray, laser scanning, and transmission electron microscopy mapping of the exopolymeric matrix of microbial biofilms. Appl. Environ. Microbiol. 69, 5543–5554.
Lawrence, J.R., Chenier, M., Roy, R., Beaumier, D., Fortin, N., Swerhone, G.D.W., Neu, T.R., Greer, C.W., 2004. Microscale and molecular assessment of the impacts of nickel, nutrients and oxygen level on river biofilm communities. Appl. Environ. Microbiol. 70, 4326–4339.
Liu, Y., Li, J., Qiu, X., Burda, C., 2007. Bactericidal activity of nitrogen-doped metal oxide nanocatalysts and the influence of bacterial extracellular polymeric substances (EPS). J Photoch. Photobio. A 190 (1), 94–100.
Lovern, S.B., Strickler, J.R., Klaper, R., 2007. Behavioral and physiological changes in *Daphnia magna* when exposed to nanoparticles suspensions (titanium dioxide, nano-C60, and C60HxC70Hx). Environ. Sci. Technol. 41 (12), 4465–4470.
Mueller, N.C., Nowack, B., 2008. Exposure modelling of engineered nanoparticles in the environment. Environ. Sci. Technol. 42 (12), 4447–4453.
Navarro, E., Baun, A., Behra, R., Hartmann, N.B., Filser, J., Miao, A.-J., Quigg, A., Santschi, P.H., Sigg, L., 2008. Environmental behavior and ecotoxicity of engineered nanoparticles to algae, plants, and fungi. Ecotoxicology 17, 372–386.
Neal, A.L., 2008. What can be inferred from bacterium-nanoparticle interactions about the potential consequences of environmental exposure to nanoparticles? Exotoxicology 17, 362–371.
Neu, T.R., Lawrence, J.R., 2009. Extracellular polymeric substances in microbial biofilm systems. Chpt 37 Microbial Glycobiology, Structures, Relevance and Applications Life Sciences edited by Anthony Moran, Patrick Brennan, Otto Holst and Mark von Itzstein. Elsevier, San Diego, CA, pp. 735–758.
Neu, T.R., Wölfl, S., Lawrence, J.R., 2004. 3-Dimensional differentiation of phototrophic biofilm constituents by multi channel confocal and 2-photon laser scanning microscopy. J. Microbiol. Meth. 56, 161–172.
Noll, F., Sumper, M., Hampp, N., 2002. Nanostructure of diatom silica surfaces and of biomimetic analogues. Nano Lett. 2, 91–95.
Obst, M., Dynes, J.J., Lawrence, J.R., Swerhone, G.D.W., Benzerara, K., Karunakaran, C., Kaznatcheev, K., Tyliszczak, T., Hitchcock, A.P., 2009. Precipitation of amorphous $CaCO_3$ (aragonite-like) by cyanobacteria: a STXM study of the influence of EPS on the nucleation process. Geochim. Cosmochim. Acta 73, 4180–4198.
Pattrick, R.A.D., van derLaan, G., Vaughan, D.J., Henderson, C.M.B., 1993. Oxidation state and electronic configuration determination of copper in tetrahedrite group minerals by *L*-edge X-ray absorption spectroscopy. Phys. Chem. Miner. 20, 395–401.
Pokrovsky, O.S., Viers, J., Emnova, E.E., Kompantseva, E.I., Freydier, R., 2008. Copper isotope fractionation during its interaction with soil and aquatic microorganisms and metal oxy(hydr)oxides: possible structural control. Geochim. Cosmochim. Acta 72, 1742–1757.
Ren, G., Hu, D., Cheng, E.W.C., Vargas-Reus, M.A., Reip, P., Allaker, R.P., 2009. Characterisation of copper oxide nanoparticles for antimicrobial applications. Int. J. Antimicrob. Agents 33, 587–590.
Thieme, J., McNulty, I., Vogt, S., Paterson, D., 2007. X-ray spectromicroscopy — a tool for environmental sciences. Environ. Sci. Technol. 41, 6885–6889.
Tiede, K., Boxall, B.A., Tearb, S.P., Lewis, J., David, H., Hassellöv, M., 2008. Detection and characterization of engineered nanoparticles in food and the environment. Food Addit. Contam. 25 (7), 795–821.
Tiede, K., Hassellöv, M., Breitbarth, E., Chaudhry, Q., Boxall, A.B.A., 2009. Considerations for environmental fate and ecotoxicity testing to support environmental risk assessments for engineered nanoparticles. J. Chromatogr. A 1216, 503–509.
Todd, E.C., Sherman, D.M., 2003. Surface oxidation of chalcocite (Cu_2S) under aqueous (pH = 2–11) and ambient atmospheric conditions: mineralogy from Cu L- and O K-edge X-ray absorption spectroscopy. Am. Mineralog. 88, 1652–1656.
Van der Laan, G., Pattrick, R.A.D., Henderson, C.M.B., Vaughan, D.J., 1992. Oxidation state variations in copper minerals studied with Cu 2p X-ray absorption spectroscopy. J. Phys. Chem. Solids. 53, 1185–1190.
WCIF (Wright Cell Imaging Facility), 2011. Image processing and analysis in JavaIt is available free for non-commercial use from http://www.uhnres.utoronto.ca/facilities/wcif/imagej/.
Wolfaardt, G.M., Lawrence, J.R., Headley, J.V., Robarts, R.D., Caldwell, D.E., 1994. Microbial exopolymers provide a mechanism for bioaccumulation of contaminants. Microb. Ecol. 27, 279–291.
Zhou, K., Wang, R., Xu, B., Li, Y., 2006. Synthesis, characterization and catalytic properties of CuO nanocrystals with various shapes. Nanotechnol. 17, 3939–3943.

Please cite this article as: Lawrence, J.R., et al., Monitoring the fate of copper nanoparticles in river biofilms using scanning transmission X-ray microscopy (STXM), Chem. Geol. (2011), doi:10.1016/j.chemgeo.2011.07.013